Ecography

ECOG-03552
McCarthy, J. K., Mokany, K., Ferrier, S. and Dwyer, J. M.2017. Predicting community rank-abundance distributions under current and future climates. – Ecography doi: 10.1111/ecog.03552

Supplementary material

Appendix 1. Queensland woody broad vegetation groups and regional ecosystems.

Here, we define our categorisation of Regional Ecosystems (REs), as defined by the Queensland Herbarium, to broad vegetation categories (Table A1). We also define how we categorised the mapped Broad Vegetation Groups (BVGs), also as defined by the Queensland Herbarium, across the study area as either woody or non-woody (Table A2). These were defined at the finest resolution available: 1:1,000,000. All analyses for this project were completed within these areas of mapped, remnant woody vegetation.

At the time of publication, the RE descriptions were available from:
https://environment.ehp.qld.gov.au/regional-ecosystems/

At the time of publication, the BVG descriptions were available as a spreadsheet from:
https://www.qld.gov.au/environment/plants-animals/plants/ecosystems/broad-vegetation/

Spatial polygons of the REs and BVGs were mapped using Version 8.0 of the Queensland Remnant Vegetation cover database. At the time of publication, this database was available at (search "Vegetation management regional ecosystem and remnant map - version 8.0"):
http://qldspatial.information.qld.gov.au/catalogue/custom/index.page

Table A1. Categorisation of the dominant Regional Ecosystems (RE1) of SEQ into broad vegetation groups (Veg. type).

RE1	Veg. type	RE1	Veg. type	RE1	Veg. type
11.10.1	sclerophyll	12.11.16x1	sclerophyll	12.12.23	sclerophyll
11.11.15	sclerophyll	12.11.17	sclerophyll	12.12.24	sclerophyll
11.11.18	rainforest	12.11.18	sclerophyll	12.12.25	sclerophyll
11.11.3	sclerophyll	12.11.18a	sclerophyll	12.12.26	sclerophyll
11.11.4	sclerophyll	12.11.19	sclerophyll	12.12.27	sclerophyll
11.11.4a	sclerophyll	12.11.2	sclerophyll	12.12.28	sclerophyll
11.11.5	rainforest	12.11.20	sclerophyll	12.12.28x1	sclerophyll
11.12.1	sclerophyll	12.11.22	sclerophyll	12.12.2a	sclerophyll
11.12.3	sclerophyll	12.11.23	sclerophyll	12.12.2b	sclerophyll
11.12.4	rainforest	12.11.3	sclerophyll	12.12.3	sclerophyll
11.12.6	sclerophyll	12.11.3a	sclerophyll	12.12.3a	sclerophyll
11.3.23	sclerophyll	12.11.3b	sclerophyll	12.12.4	sclerophyll
11.3.25	sclerophyll	12.11.4	rainforest	12.12.5	sclerophyll
11.3.26	sclerophyll	12.11.5a	sclerophyll	12.12.6	sclerophyll
11.3.29	sclerophyll	12.11.5e	sclerophyll	12.12.7	sclerophyll
11.3.4	sclerophyll	12.11.5h	sclerophyll	12.12.8	sclerophyll
11.5.15	rainforest	12.11.5j	sclerophyll	12.12.9	sclerophyll
11.5.2	sclerophyll	12.11.5k	sclerophyll	12.2.1	rainforest
11.5.20	sclerophyll	12.11.6	sclerophyll	12.2.10	sclerophyll
11.7.4c	sclerophyll	12.11.7	sclerophyll	12.2.11	sclerophyll
11.7.6	sclerophyll	12.11.8	sclerophyll	12.2.12	heath
11.8.2a	sclerophyll	12.11.9	sclerophyll	12.2.13	heath
11.8.3	rainforest	12.11.9x1	sclerophyll	12.2.14	sclerophyll
11.8.4	sclerophyll	12.12.1	rainforest	12.2.14a	sclerophyll
11.8.5	sclerophyll	12.12.10	heath	12.2.14b	sclerophyll
11.8.5a	sclerophyll	12.12.11	sclerophyll	12.2.14c	sclerophyll
11.8.8	sclerophyll	12.12.12	sclerophyll	12.2.14e	grassland
11.9.13	sclerophyll	12.12.13	rainforest	12.2.14f	grassland
11.9.2	sclerophyll	12.12.14	sclerophyll	12.2.14g	grassland
11.9.4c	rainforest	12.12.15	sclerophyll	12.2.14h	grassland
11.9.9	sclerophyll	12.12.15a	sclerophyll	12.2.15	wetland
12.1.1	sclerophyll	12.12.15b	sclerophyll	12.2.15a	wetland
12.1.2	grassland	12.12.16	rainforest	12.2.15f	wetland
12.1.3	mangrove	12.12.17	rainforest	12.2.16	sand
12.11.1	rainforest	12.12.18	rainforest	12.2.17a	grassland
12.11.10	rainforest	12.12.19	sclerophyll	12.2.17b	grassland
12.11.11	rainforest	12.12.19x2	sclerophyll	12.2.17c	wetland
12.11.12	rainforest	12.12.19x3	sclerophyll	12.2.18a	grassland
12.11.13	rainforest	12.12.2	sclerophyll	12.2.18b	grassland
12.11.14	sclerophyll	12.12.20	sclerophyll	12.2.18c	grassland
12.11.15	sclerophyll	12.12.21	sclerophyll	12.2.19a	sclerophyll
12.11.16	sclerophyll	12.12.22	sclerophyll	12.2.19b	sclerophyll
12.2.19c	sclerophyll	12.3.9	sclerophyll	12.8.21	rainforest
12.2.19d	sclerophyll	12.5.1	sclerophyll	12.8.22	rainforest

RE1	Veg. type
12.2.2	rainforest
12.2.20a	sclerophyll
12.2.20b	sclerophyll
12.2.21a	rainforest
12.2.21b	rainforest
12.2.21c	rainforest
12.2.21d	rainforest
12.2.3	rainforest
12.2.4	rainforest
12.2.5	sclerophyll
12.2.6	sclerophyll
12.2.7	sclerophyll
12.2.7a	sclerophyll
12.2.7c	sclerophyll
12.2.8	sclerophyll
12.2.9	heath
12.3.1	rainforest
12.3.10	sclerophyll
12.3.10a	sclerophyll
12.3.11	sclerophyll
12.3.11a	sclerophyll
12.3.12	sclerophyll
12.3.13	heath
12.3.14	sclerophyll
12.3.14a	sclerophyll
12.3.15	sclerophyll
12.3.2	sclerophyll
12.3.3	sclerophyll
12.3.3a	sclerophyll
12.3.3b	sclerophyll
12.3.3c	sclerophyll
12.3.3d	sclerophyll
12.3.4	sclerophyll
12.3.4a	sclerophyll
12.3.5	sclerophyll
12.3.5a	sclerophyll
12.3.6	sclerophyll
12.3.7	sclerophyll
12.3.7a	sclerophyll
12.3.7b	wetland
12.3.7c	wetland
12.3.7d	wetland
12.3.8	wetland
12.9-10.5	sclerophyll
12.9-10.5a	sclerophyll
12.9-10.5b	sclerophyll
12.9-10.5c	sclerophyll

RE1	Veg. type
12.5.10	sclerophyll
12.5.11	sclerophyll
12.5.12	sclerophyll
12.5.13a	rainforest
12.5.13b	rainforest
12.5.13c	rainforest
12.5.1a	sclerophyll
12.5.1b	sclerophyll
12.5.1c	sclerophyll
12.5.1e	sclerophyll
12.5.2a	sclerophyll
12.5.2b	sclerophyll
12.5.3	sclerophyll
12.5.3a	sclerophyll
12.5.4	sclerophyll
12.5.4a	sclerophyll
12.5.5	sclerophyll
12.5.6	sclerophyll
12.5.6a	sclerophyll
12.5.6b	sclerophyll
12.5.6c	sclerophyll
12.5.7	sclerophyll
12.5.7a	sclerophyll
12.5.8	sclerophyll
12.5.9	heath
12.5.9a	heath
12.7.1	sclerophyll
12.7.2	sclerophyll
12.8.1	sclerophyll
12.8.10	sclerophyll
12.8.11	sclerophyll
12.8.12	sclerophyll
12.8.13	rainforest
12.8.14	sclerophyll
12.8.14a	sclerophyll
12.8.15	grassland
12.8.16	sclerophyll
12.8.17	sclerophyll
12.8.18	rainforest
12.8.19	heath
12.8.1a	sclerophyll
12.8.2	sclerophyll
12.8.20	sclerophyll
12.9-10.7a	sclerophyll
12.9-10.8	sclerophyll
12.9-10.9	sclerophyll
canal	wetland

RE1	Veg. type
12.8.23	sclerophyll
12.8.24	sclerophyll
12.8.25	sclerophyll
12.8.26	sclerophyll
12.8.3	rainforest
12.8.4	rainforest
12.8.5	rainforest
12.8.6	rainforest
12.8.7	rainforest
12.8.8	sclerophyll
12.8.8a	sclerophyll
12.8.9	rainforest
12.9-10.1	sclerophyll
12.9-10.11	sclerophyll
12.9-10.11a	sclerophyll
12.9-10.12	sclerophyll
12.9-10.12a	sclerophyll
12.9-10.13	sclerophyll
12.9-10.14	sclerophyll
12.9-10.14a	sclerophyll
12.9-10.14b	sclerophyll
12.9-10.15	rainforest
12.9-10.16	rainforest
12.9-10.17	sclerophyll
12.9-10.17a	sclerophyll
12.9-10.17b	sclerophyll
12.9-10.17c	sclerophyll
12.9-10.17d	sclerophyll
12.9-10.17e	sclerophyll
12.9-10.18	sclerophyll
12.9-10.18a	sclerophyll
12.9-10.18b	sclerophyll
12.9-10.19	sclerophyll
12.9-10.19a	sclerophyll
12.9-10.1x1	sclerophyll
12.9-10.2	sclerophyll
12.9-10.20	sclerophyll
12.9-10.21	sclerophyll
12.9-10.22	heath
12.9-10.23	sclerophyll
12.9-10.24	sclerophyll
12.9-10.3	sclerophyll
12.9-10.4	sclerophyll
non-rem	non-rem
ocean	wetland
plant	plantation
sand	sand

RE1	Veg. type
12.9-10.5d	sclerophyll
12.9-10.6	sclerophyll
12.9-10.7	sclerophyll

RE1	Veg. type
estuary	wetland
hoop	plantation

RE1	Veg. type
small_i	sand
water	wetland

Table A2. Categorisation of the mapped Broad Vegetation Groups (BVGs) codes of SEQ as either woody or non-woody ecosystems.

BVG	Ecosystem	BVG	Ecosystem	BVG	Ecosystem
1a	Woody	12b	Woody	23b	Woody
1b	Woody	13a	Woody	24a	Woody
2a	Woody	13b	Woody	24b	Woody
2b	Woody	13c	Woody	25a	Woody
2c	Woody	13d	Woody	26a	Woody
2d	Woody	14a	Woody	27a	Woody
3a	Woody	14b	Woody	27b	Woody
4a	Woody	14c	Woody	27c	Woody
4b	Woody	14d	Woody	28a	Woody
5a	Woody	15a	Woody	28b	Woody
5b	Woody	15b	Woody	28c	Woody
5c	Woody	16a	Woody	28d	Non-woody
5d	Woody	16b	Woody	28e	Woody
6a	Woody	16c	Woody	29a	Woody
6b	Woody	16d	Non-woody	29b	Woody
7a	Woody	17a	Woody	30a	Non-woody
7b	Woody	17b	Woody	30b	Non-woody
8a	Woody	17c	Woody	31a	Non-woody
8b	Woody	18a	Woody	31b	Non-woody
9a	Woody	18b	Woody	32a	Non-woody
9b	Woody	18c	Woody	32b	Non-woody
9c	Woody	18d	Woody	33a	Non-woody
9d	Woody	19a	Woody	33b	Non-woody
9e	Woody	19b	Woody	34a	Non-woody
9f	Woody	19c	Woody	34b	Non-woody
9g	Woody	19d	Woody	34c	Non-woody
9h	Woody	20a	Woody	34d	Non-woody
10a	Woody	21a	Woody	34e	Non-woody
10b	Woody	21b	Woody	34f	Non-woody
11a	Woody	22a	Woody	34g	Non-woody
11b	Woody	22b	Woody	35a	Woody
11c	Woody	22c	Woody	35b	Non-woody
12a	Woody	23a	Woody		

Appendix 2. Environmental variables used to derive and predict rank-abundance distribution (RAD) models under current and future climates.

Here we present the environmental variables used to predict RADs across SEQ. All 32 environmental variables available were used during the model selection process and 17 were selected in at least one of the final RAD models (Figs A1 & A2, Table A1). All variables were standardised prior to analyses and future layers were standardised against the mean and standard deviations of their current versions.

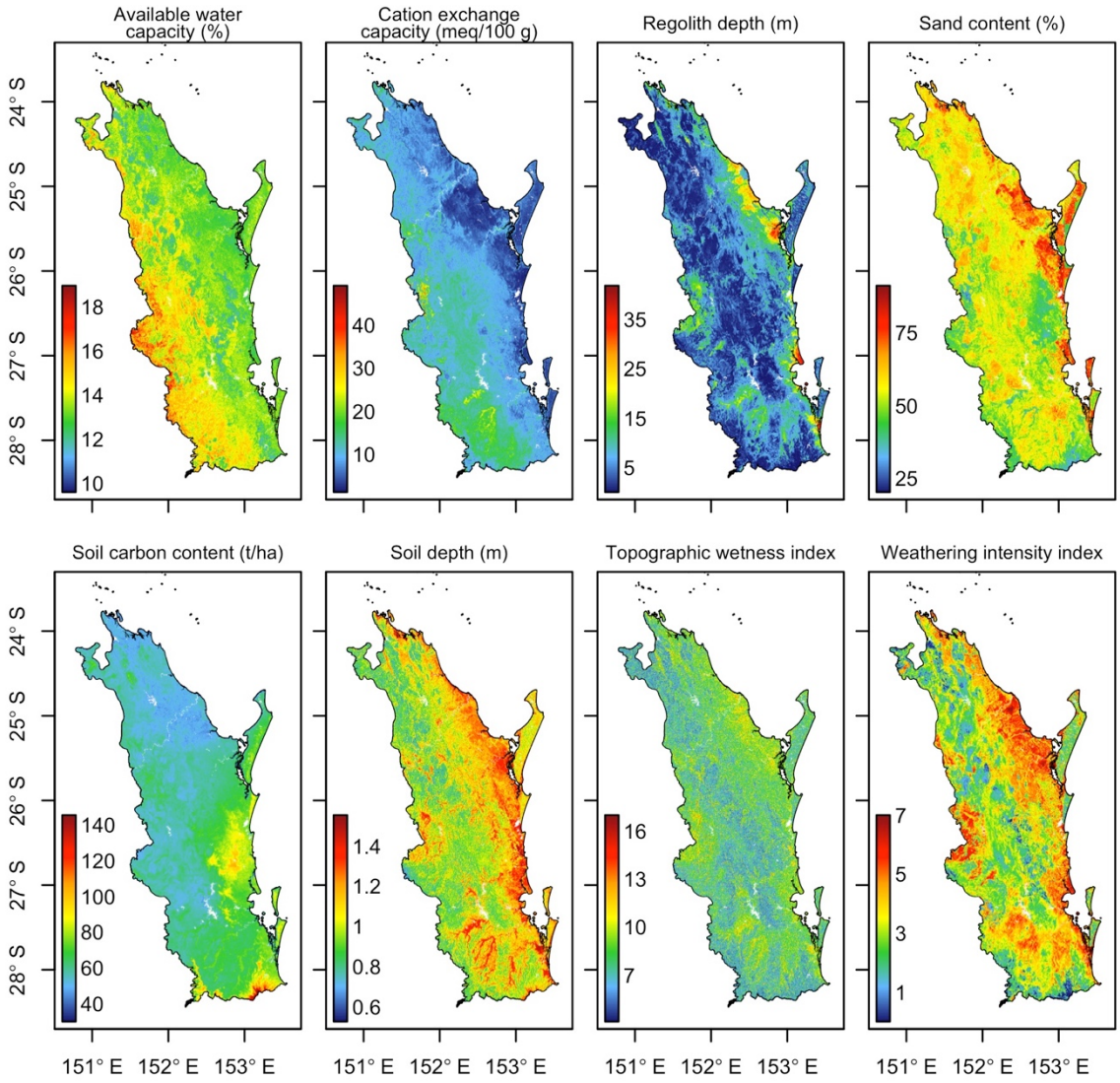

Figure A1. Substrate and vegetation variables included in at least one of the final RAD models. Note that while the raw versions are presented here, standardised versions were used at all stages of the modelling process. Fire frequency was also included all three RAD models; this variable presented in Appendix 3.

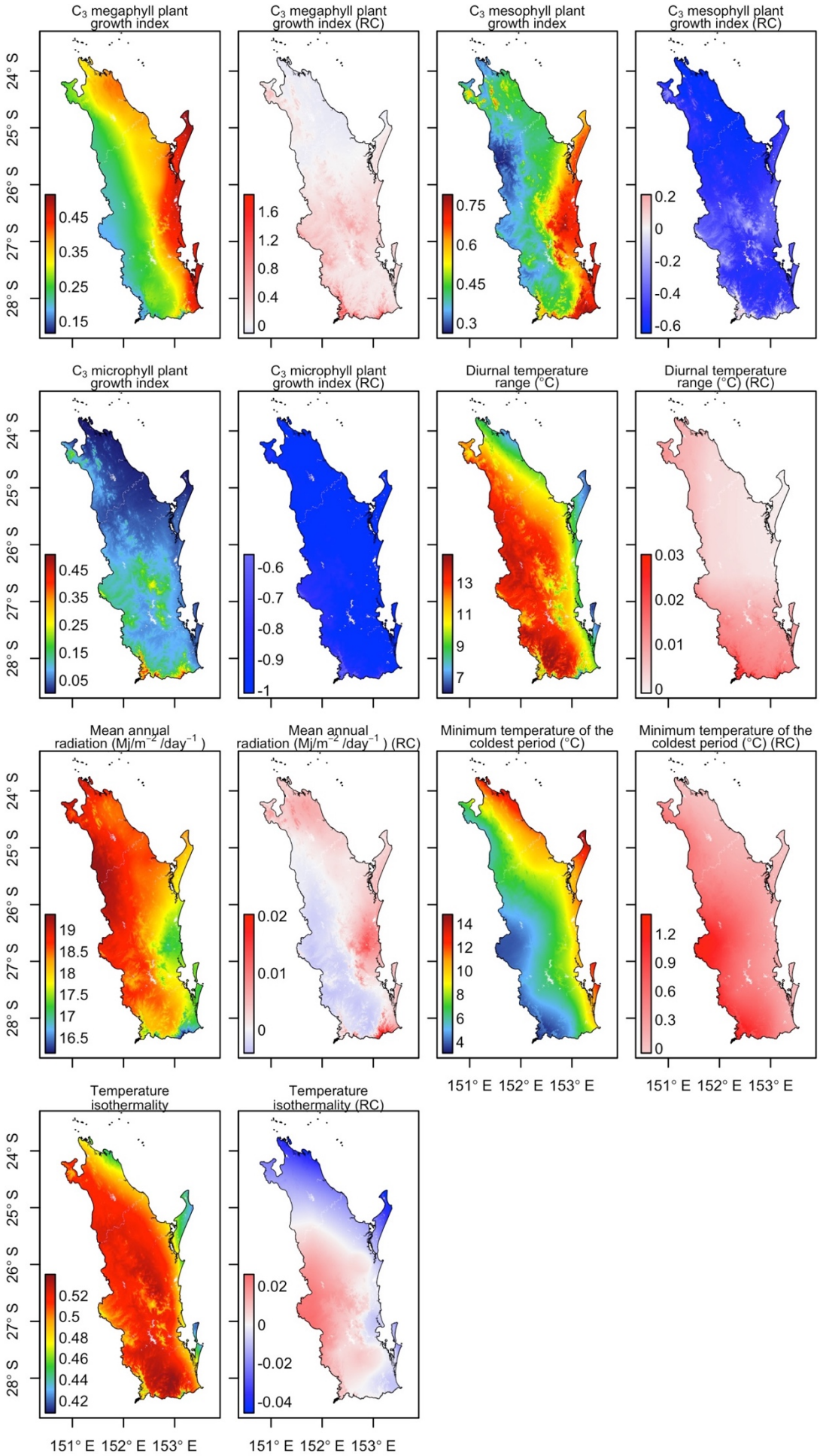
C3 megaphyll plant growth index
C3 megaphyll plant growth index (RC)
C3 mesophyll plant growth index
C3 mesophyll plant growth index (RC)
C3 microphyll plant growth index
C3 microphyll plant growth index (RC)
Diurnal temperature range (°C)
Diurnal temperature range (°C) (RC)
Mean annual radiation (Mj/m-2 /day-1)
Mean annual radiation (Mj/m-2 /day-1) (RC)
Minimum temperature of the coldest period (°C)
Minimum temperature of the coldest period (°C) (RC)
Temperature isothermality
Temperature isothermality (RC)
24° S
25° S
26° S
27° S
28° S
151° E 152° E 153° E

Figure A2. All climate and vegetation variables included in at least one of the final RAD models. For each variable, the current version and the relative change (RC) of the future version are displayed for each version. Note that while the raw versions are presented here, standardised versions were used at all stages of the modelling process. Vegetation height was also included the abundance and richness models; this variable presented in Appendix 4.

Table A1. Descriptions of environmental variables used during the model selection process for RAD models. Variables selected in one (or more) of the models are indicated in bold. All climate models were projected into the future using the CanESM2 and RCP8.5 for 2090.

Environmental variable	Broad category	Unit	Short description	Reference
Annual evaporation	Climate	mm	Mean annual potential evapotranspiration.	Xu & Hutchinson (2011)
Annual precipitation	Climate	mm	Mean annual precipitation.	Xu & Hutchinson (2011)
Available water capacity	Substrate	%	The available water capacity of the surface soil (0-50 mm).	Viscarra Rossel et al. (2014a)
C_3 megaphyll plant growth index	Vegetation	No unit	Yearly mean growth index (range 0 to 1) from simple plant growth model for C_3 megaphyll plant type using data on temperature, precipitation, evaporation and radiation across a year.	Xu & Hutchinson (2011)
C_3 mesophyll plant growth index	Vegetation	No unit	Yearly mean growth index (range 0 to 1) from simple plant growth model for C_3 mesophyll plant type using data on temperature, precipitation, evaporation and radiation across a year.	Xu & Hutchinson (2011)
C_3 microphyll plant growth index	Vegetation	No unit	Yearly mean growth index (range 0 to 1) from simple plant growth model for C_3 microphyll plant type using data on temperature, precipitation, evaporation and radiation across a year.	Xu & Hutchinson (2011)
C_4 megaphyll plant growth index	Vegetation	No unit	Yearly mean growth index (range 0 to 1) from simple plant growth model for C_4 megaphyll plant type using data on temperature, precipitation, evaporation and radiation across a year.	Xu & Hutchinson (2011)
Clay content	Substrate	%	The clay content of the surface soil (0-50 mm).	Viscarra Rossel et al. (2014b)

Environmental variable	Broad category	Unit	Short description	Reference
Diurnal temperature range	Climate	°C	The mean over the whole year of the weekly diurnal temperature ranges. Each weekly diurnal range is the difference between that week's maximum and minimum temperature.	Xu & Hutchinson (2011)
Effective cation exchange capacity	Substrate	meq/100 g	The total capacity of the surface soil (0-50 mm) to hold exchangeable cations; provides a measure of a soil's ability to hold essential nutrients and provides a buffer against soil acidification.	Viscarra Rossel et al. (2014c)
Fire frequency	Vegetation	Years	The number of years a fire-scar was identified from satellite imagery between 1987 and 2014.	Appendix 3
Maximum temperature of the warmest period	Climate	°C	The highest maximum temperature in all weeks of the year.	Xu & Hutchinson (2011)
Mean annual radiation	Climate	$Mj.m^{-2}.day^{-1}$	Annual mean daily radiation	Xu & Hutchinson (2011)
Mean annual temperature	Climate	°C	The mean of all weekly mean temperatures.	Xu & Hutchinson (2011)
Minimum temperature of the coolest period	Climate	°C	The lowest minimum temperature in all weeks of the year.	Xu & Hutchinson (2011)
Nitrogen content	Substrate	%	The nitrogen content of the surface soil (0-50 mm).	Viscarra Rossel et al. (2014d)
pH – $CaCl_2$	Substrate	None	pH of 1:5 soil/0.01 M calcium chloride extract.	Viscarra Rossel et al. (2014e)
Phosphorus content	Substrate	%	The phosphorus content of the surface soil (0-50 mm).	Viscarra Rossel et al. (2014f)
Precipitation:PET ratio	Climate	Ratio	Annual precipitation divided by annual potential evapotranspiration (PET)	Xu & Hutchinson (2011)

Appendix 2 references

Gallant, J. C. and Austin, J. (2012a) Prescott Index derived from 1" SRTM DEM-S. v2. CSIRO Data Collection. http://doi.org/10.4225/08/53EB2D0EAE377

Gallant, J. C. and Austin, J. (2012b) Topographic Wetness Index derived from 1" SRTM DEM-H. v2. CSIRO. Data Collection. http://doi.org/10.4225/08/57590B59A4A08

Viscarra Rossel, R. A. et al. (2014a). Soil and Landscape Grid National Soil Attribute Maps – Available Water Capacity (3" resolution) – Release 1. v1. CSIRO. Data Collection. http://doi.org/10.4225/08/546ED604ADD8A

Viscarra Rossel, R. A. et al. (2014b). Soil and Landscape Grid National Soil Attribute Maps – Clay (3" resolution) – Release 1. v4. CSIRO. Data Collection. http://doi.org/10.4225/08/546EEE35164BF

Viscarra Rossel, R. A. et al. (2014c). Soil and Landscape Grid National Soil Attribute Maps – Effective Cation Exchange Capacity (3" resolution) – Release 1. v3. CSIRO. Data Collection. http://doi.org/10.4225/08/546F091C11777

Viscarra Rossel, R. A. et al. (2014d). Soil and Landscape Grid National Soil Attribute Maps – Total Nitrogen (3" resolution) – Release 1. v4. CSIRO. Data Collection. http://doi.org/10.4225/08/546F564AE11F9

Viscarra Rossel, R. A. et al. (2014e). Soil and Landscape Grid National Soil Attribute Maps – pH - CaCl2 (3" resolution) – Release 1. v2. CSIRO. Data Collection. http://doi.org/10.4225/08/546F17EC6AB6E

Viscarra Rossel, R. A. et al. (2014f). Soil and Landscape Grid National Soil Attribute Maps – Total Phosphorus (3" resolution) – Release 1. v4. CSIRO. Data Collection. http://doi.org/10.4225/08/546F617719CAF

Viscarra Rossel, R. A. et al. (2014g). Soil and Landscape Grid National Soil Attribute Maps – Silt (3" resolution) – Release 1. v4. CSIRO. Data Collection. http://doi.org/10.4225/08/546F48D6A6D48

Viscarra Rossel, R. A. et al. (2014h). Soil and Landscape Grid National Soil Attribute Maps – Sand (3" resolution) – Release 1. v4. CSIRO. Data Collection. http://doi.org/10.4225/08/546F29646877E

Viscarra Rossel, R. A. et al. (2014i). Soil and Landscape Grid National Soil Attribute Maps – Bulk Density - Whole Earth (3" resolution) – Release 1. v4. CSIRO. Data Collection. http://doi.org/10.4225/08/546EE212B0048

Viscarra Rossel, R. A. et al. 2014. Baseline map of organic carbon in Australian soil to support national carbon accounting and monitoring under climate change. — Global Change Biol. 20: 2953-2970.

Viscarra Rossel, R. A. et al. (2014k). Soil and Landscape Grid National Soil Attribute Maps – Soil Depth (3" resolution) – Release 1. v2. CSIRO. Data Collection. http://doi.org/10.4225/08/546F540FE10AA

Wilford, J. 2012. A weathering intensity index for the Australian continent using airborne gamma-ray spectrometry and digital terrain analysis. — Geoderma 183: 124-142.

Wilford, J. et al. (2015): Soil and Landscape Grid National Soil Attribute Maps – Depth of Regolith (3" resolution) – Release 2. v5. CSIRO. Data Collection. http://doi.org/10.4225/08/55C9472F05295

Xu, T. and Hutchinson, M. 2010. ANUCLIM Version 6.1 user guide. — Fenner School of Environment and Society, The Australian National University.

Appendix 3. Generating the fire frequency layer.

In order to generate a layer to capture the frequency of fire occurrence across southeast Queensland we utilised the Landsat fire scars Queensland series measured yearly from 1987-2014 (Department of Science, Information Technology and Innovation 2016). These data are available across our entire study area and identify visibly blackened land surfaces caused by fire from Landsat imagery with an accuracy of 85% (Goodwin & Collett 2014). These data are available as annual layers with values indicating the month when a fire scar was first detected. For our purposes, we reduced the temporal component to a simple binary 0 (no fire detected during annual cycle) or 1 (fire detected) indicating whether a fire occurred in a particular pixel in that year. The resolution of the Landsat-derived fire scar data (30 m) was finer than the other environmental variables we include in this study (90 m). As such, we resampled each yearly fire scar layer from our template layer extracting the fire scar value that was recorded nearest the centre of each 90 m pixel/cell. The fire frequency layer we use here was a sum of each of these resampled yearly layers giving an indication of fire frequency across 28 years of available data (Fig. A1).

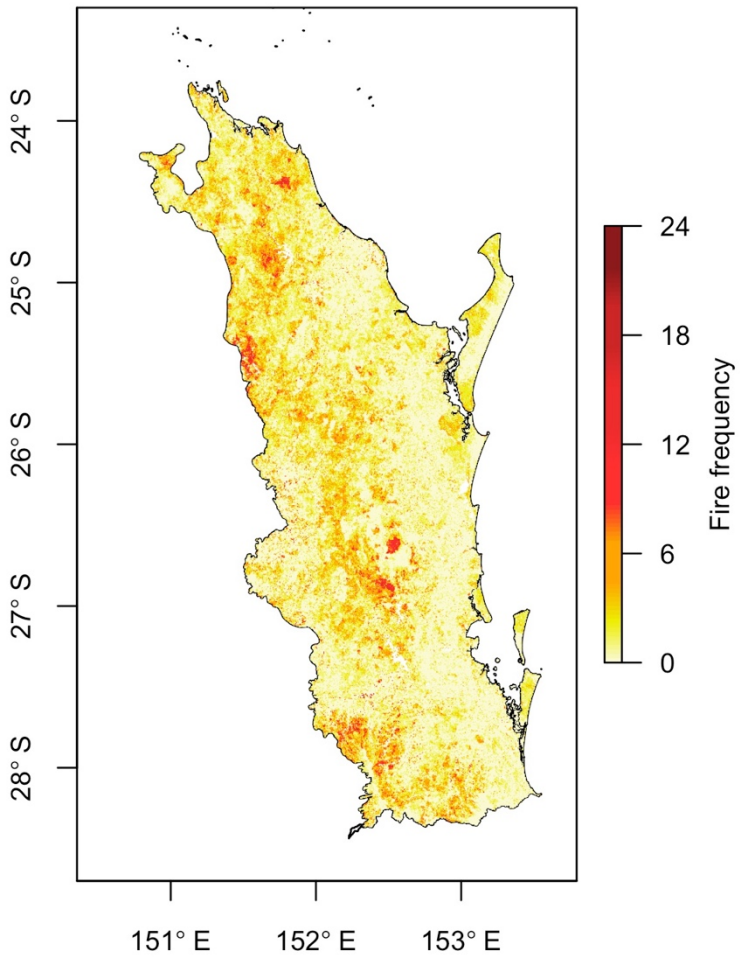

Figure A1. A measure of fire frequency across south east Queensland was generated from 28 annual fire-scar layers derived from Landsat imagery.

Appendix 3 references

Department of Science, Information Technology and Innovation (2016) Landsat fire scars Queensland series. Available at: http://www.qld.gov.au/environment/land/vegetation/mapping/firescar-maps/ (accessed 2 March 2016).

Goodwin, N. R. and Collett, L. J. 2014. Development of an automated method for mapping fire history captured in Landsat TM and ETM+ time series across Queensland, Australia. — Remote Sens. Environ. 148: 206-221.

Appendix 4. Generating the vegetation height layer.

To predict the maximum height of the vegetation across southeast Queensland (SEQ) we utilised the median height of the tallest stratum (measured in m) measured in the Queensland Herbarium's CORVEG dataset (1,718 sites, see main text and Neldner et al. 2012) and 30 additional sites collected in 2016 using the same methodology (McCarthy et al. 2016) (total, 1,748 sites). A multiple regression analysis was used to estimate the maximum height of the vegetation using a linear model. Linear and quadratic relationships were considered and model selection was conducted using forward selection based on Akaike information criterion (AIC) and 31 standardised explanatory variables (covariates, Appendix 2). Relationships between selected variables were visually assessed at each step with unrealistic or weakly-supported relationships not included in the final model. As many of our environmental variables exhibit some level of collinearity, variables with a correlation of $\geq$ 0.6 with a previously selected variable were not included. Models within two AIC units of the previous model were considered to have equivalent explanatory power after which no more terms were added. All possible interactions between selected linear terms were then added using forward selection and AIC. The final model included seven covariates, three of which were linear and four quadratic (Table A1). No interactions were selected. Vegetation height was found to increase with temperature isothermality and available water capacity and decrease with pH (quadratic), sand content and fire frequency (quadratic) ($F_{11, 1745} = 86.37$, $P < 0.001$, $R^2 = 0.35$) (Figure A1). Vegetation height had quadratic relationships with soil depth and annual evaporation with increased height at moderate soil depth and extreme levels (high and low) of annual evaporation.

This model was used to estimate the maximum vegetation height across SEQ at a resolution of 90 m and negative predicted heights were set to zero. Areas of tall vegetation were correctly predicted in the southern forests of Main Range and Lamington National Parks, and north through wet-sclerophyll areas like Conondale National Park and the northern rainforests (Figure A2a). Areas of short vegetation were predicted to occur along the coast where shrubby heath ecosystems dominate, as well as inland areas of montane heath and stunted woodlands. Future climate variables (Table A1) were derived for the year 2090 using the CanESM2 and RCP8.5 and standardised against the mean and standard deviation of the current climate layers. The extremes (maximum and minimum) of the future climate variables were clamped to the extremes of their current versions to prevent unrealistic predictions into unsampled climate space. This climate future represents a worst-case scenario with marked increases in temperature, evaporation, precipitation and radiation across most of SEQ. These future climate layers (and unchanged substrate layers) were used to estimate the potential maximum height of vegetation in the future. Most of SEQ was predicted to increase in height, up to 6 m in some areas. Areas in the far-north and –south, including Lamington and Main Range National Parks, although still predicted to carry tall forest, were predicted to become shorter with decreases in height of up to 4 m in some areas (Figure A2b, c).

Table A1. Summary of forward model selection and effect of standardised covariates included in the linear-model used to predict the vegetation height layer. Bold values denote statistical significance at $P < 0.05$.

Environmental covariate	No. parameters	AIC	Estimate	SE	t	*P*
Intercept		12,028.84	22.14	0.31	70.36	**< 0.001**
Soil depth			-1.49	0.17	-8.98	**< 0.001**
Soil depth^2	2	11,605.02	-1.23	0.10	-12.09	**< 0.001**
*Temperature isothermality	3	11,430.65	2.33	0.17	13.34	**< 0.001**
Sand content	4	11.349.91	-1.32	0.17	-7.84	**< 0.001**
pH – $CaCl_2$			-2.16	0.29	-7.14	**< 0.001**
pH – $CaCl_2^2$	6	11,315.75	-0.52	0.17	-3.00	**0.003**
*Annual evaporation			0.82	0.19	4.29	**< 0.001**
*Annual evaporation^2	8	11,304.49	0.39	0.12	3.28	**0.001**
Available water capacity	9	11,291.11	0.75	0.19	3.96	**< 0.001**
Fire frequency			-0.15	0.26	-0.58	0.563
Fire frequency^2	11	11,287.11	-0.33	0.16	-2.07	**0.038**

*Denotes a climate variable that was projected using the CanESM2 and RCP8.5 for 2090 to estimate the future maximum height of vegetation under a changing climate.

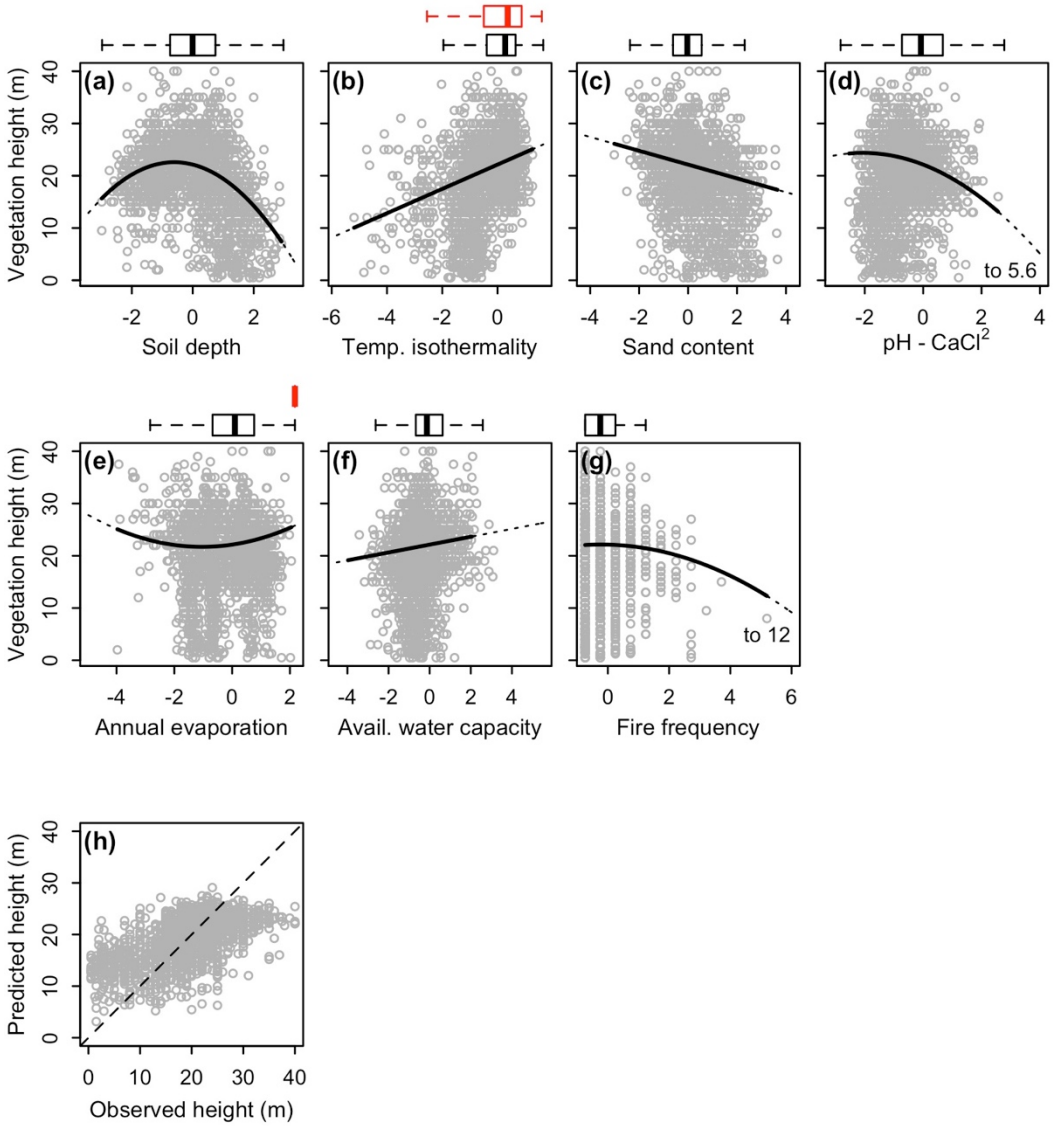

Figure A1. The maximum vegetation height was estimated across southeast Queensland using seven standardised environmental covariates (a-g). The solid lines are fitted relationships within sampled environmental space. Dotted lines extend into unsampled climate space. Box plots (outliers not shown) show the distribution of predictor variables under current (black) and future (red, where appropriate) climates. Note that future climate variables are clamped at the extremes of their current versions to reduce predicting into unsampled environmental space (see main text). The median height of the tallest stratum from 1,748 sites in SEQ was used to inform the model (h).

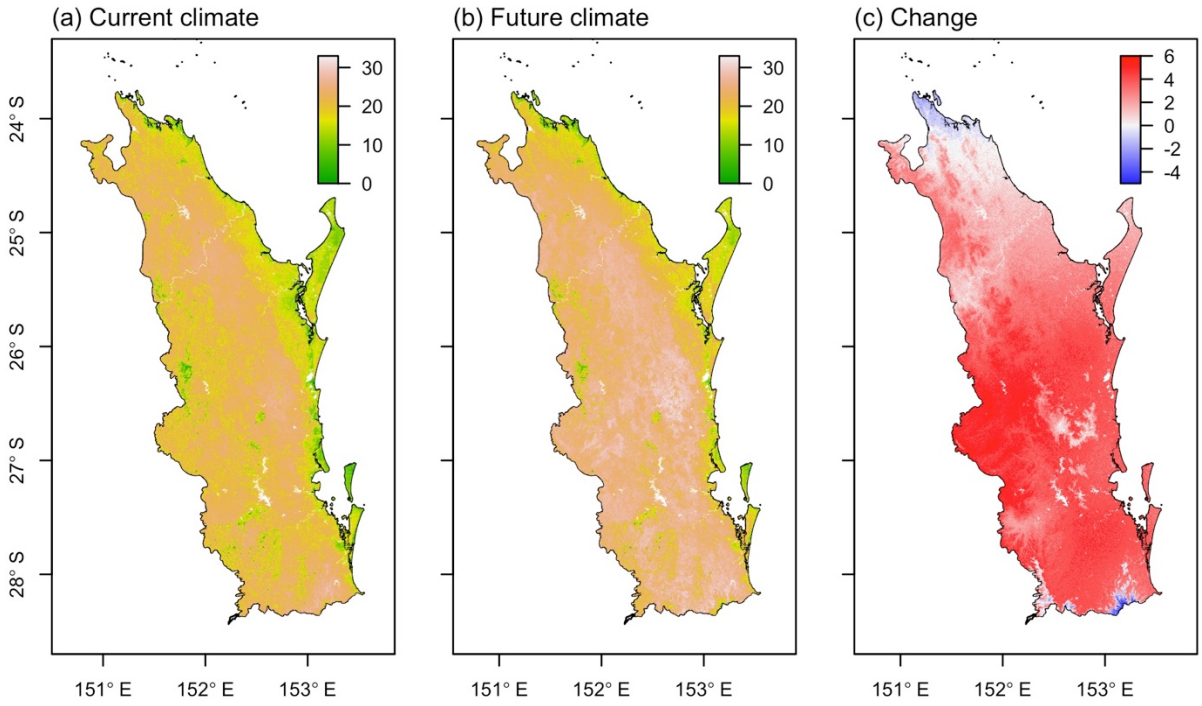

Figure A2. The predicted maximum height of vegetation (m) across southeast Queensland was generated under current and future climates (a-b) and the climate-induced change (c).

Appendix 4 references

McCarthy, J. K. et al. 2016. Estimating plant abundances from crown cover and forest structure data reveals size-dependent patterns of rarity in subtropical Australia. — Appl. Veg. Sci. 19: 700-710.

Neldner, V. J. et al. 2012. Methodology for Survey and Mapping of Regional Ecosystems and Vegetation Communities in Queensland. — Queensland Herbarium, Queensland Department of Science, Information Technology, Innovation and the Arts.

Appendix 5. Justification for selecting 500 bootstrap samples when predicting RADs.

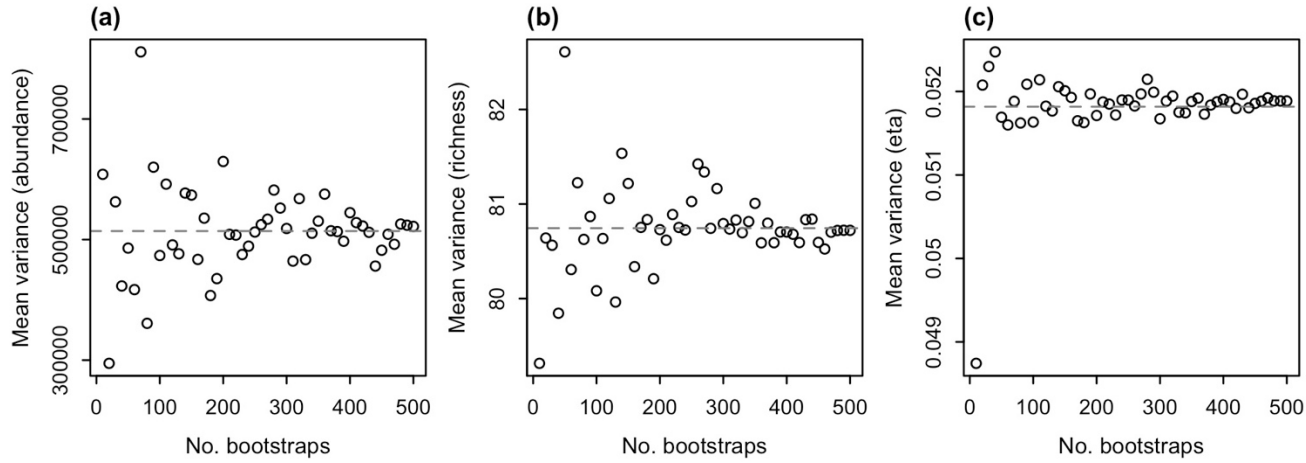

Figure A1. Due to the computational resources required to predict from the RAD package, we were limited in the number of bootstrap samples we could perform. A super-computer cluster was required to run these analyses and, as such, computing time was limited. We tested whether 500 bootstraps would be sufficient by simulating predictions using between 10 and 500 bootstraps (increasing by iterations of 10 bootstraps) and ensuring that the variance in predictions stabilised at the maximum 500. The dashed horizontal lines indicate the mean variance across the entire simulation.

Appendix 6. Summary of RAD models including selection and effect of covariates.

Table A1. Summary of model selection and effect of covariates included in each of the three components of the RAD model (abundance, richness and relative abundance) for woody plants in southeast Queensland. All environmental covariates were standardised prior to fitting the models.

Covariate	Estimate	AIC
(a) Total abundance, N_i		
Dispersion (θ_N)	1.17	
Intercept	5.15	22,699.08
C_3 megaphyll	-0.26	
C_3 megaphyll^2	0.13	22,621.55
Sand content	0.09	
Sand content^2	0.08	22,585.41
Vegetation height	0.17	
Vegetation height^2	0.02	22,522.12
Fire frequency	-0.28	22,504.51
Soil carbon content	0.25	22,490.57
Weathering intensity index	0.04	22,483.55
Temperature isothermality	-0.17	22,475.97
C_3 microphyll	-0.02	
C_3 microphyll^2	-0.08	22,471.23
Soil carbon content:weathering intensity index	-0.13	22,439.88
Fire frequency:temperature isothermality	-0.15	22,421.94
Weathering intensity index:temperature isothermality	-0.09	22,409.69
(b) Richness, $S_i\|N_i$		
Dispersion (θ_S)	12.56	
Intercept	0.05	8,156.10
log(N_i)	0.47	7,181.55
Regolith depth	-0.06	
Regolith depth^2	-0.01	7,088.79
Diurnal temperature range	-0.17	
Diurnal temperature range^2	-0.06	7,060.54
Vegetation height	0.01	
Vegetation height^2	-0.01	7,034.69
Effective cation exchange capacity	0.02	
Effective cation exchange capacity^2	-0.04	7,024.72
Mean annual radiation	0.09	7,014.11
Fire frequency	-0.07	7,003.17
Sand content	-0.08	6,993.22
Topographic wetness index	0.04	
Topographic wetness index^2	-0.03	6,985.65
(c) Evenness, $n_i\|N_i, S_i$		
Dispersion (θ_n)	10.25	
Dispersion (ν)	2.01	
Intercept	1.20	72,719.76

Covariate	**Estimate**	**AIC**
log(N_i)	0.25	71,720.79
log(S_i)	-0.52	71,648.70
Minimum temperature of the coolest period	-0.07	
Minimum temperature of the coolest period^2	-0.01	71,564.31
Soil depth	0.01	
Soil depth^2	-0.03	71,525.67
C_3 mesophyll	0.08	
C_3 mesophyll^2	-0.05	71,481.49
Available water capacity	-0.04	
Available water capacity^2	-0.02	71,465.86
Sand content	-0.03	
Sand content^2	0.01	71,458.20
Fire frequency	-0.01	
Fire frequency^2	-0.02	71,455.35

Appendix 7. Coefficient plots for the abundance, richness and evenness models.

Here we present the coefficient plots for the three components of the RAD model: abundance (Fig. A1), richness (Fig. A2) and evenness (Fig. A3). All environmental predictor variables were standardised prior to fitting the models.

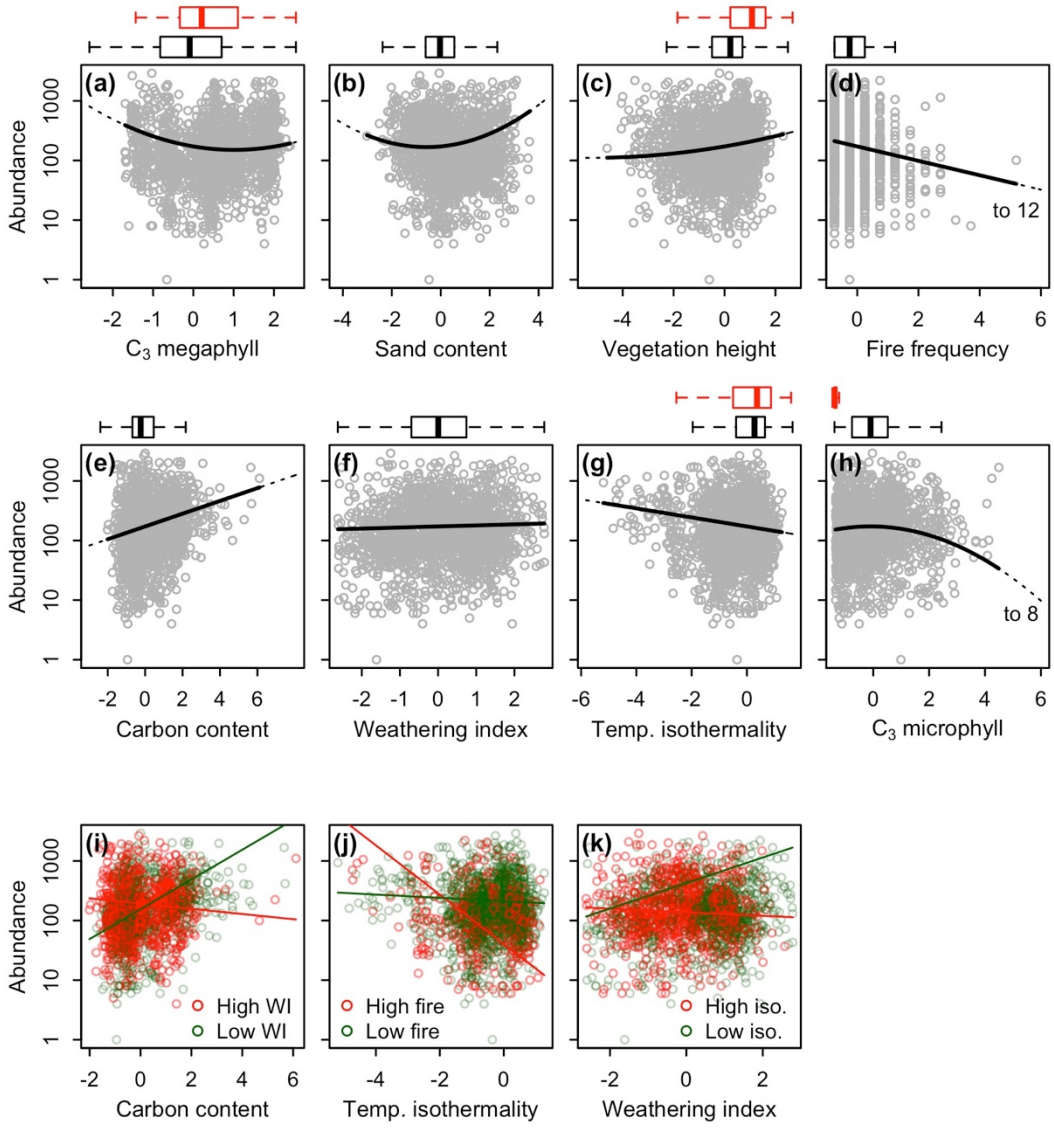

Figure A1. Eight standardised predictor variables were selected for the abundance model (a-h) as well as three interactions: (i) carbon content and weathering intensity index, (j) temperature isothermality and fire frequency and (k) weathering intensity index and temperature isothermality. The solid lines are fitted relationships within sampled environmental space. Dotted lines extend into unsampled climate space. Box plots (outliers not shown) show the distribution of predictor variables under current (black) and future (red, where appropriate) climates. Note that future climate variables are clamped at the extremes of their current versions to reduce predicting into unsampled environmental space (see main text). Abundance values indicate the number of stems per 1000 m^2 plot; note that these values (the y-axis) are plotted on the $\log_e$ scale to aid interpretation.

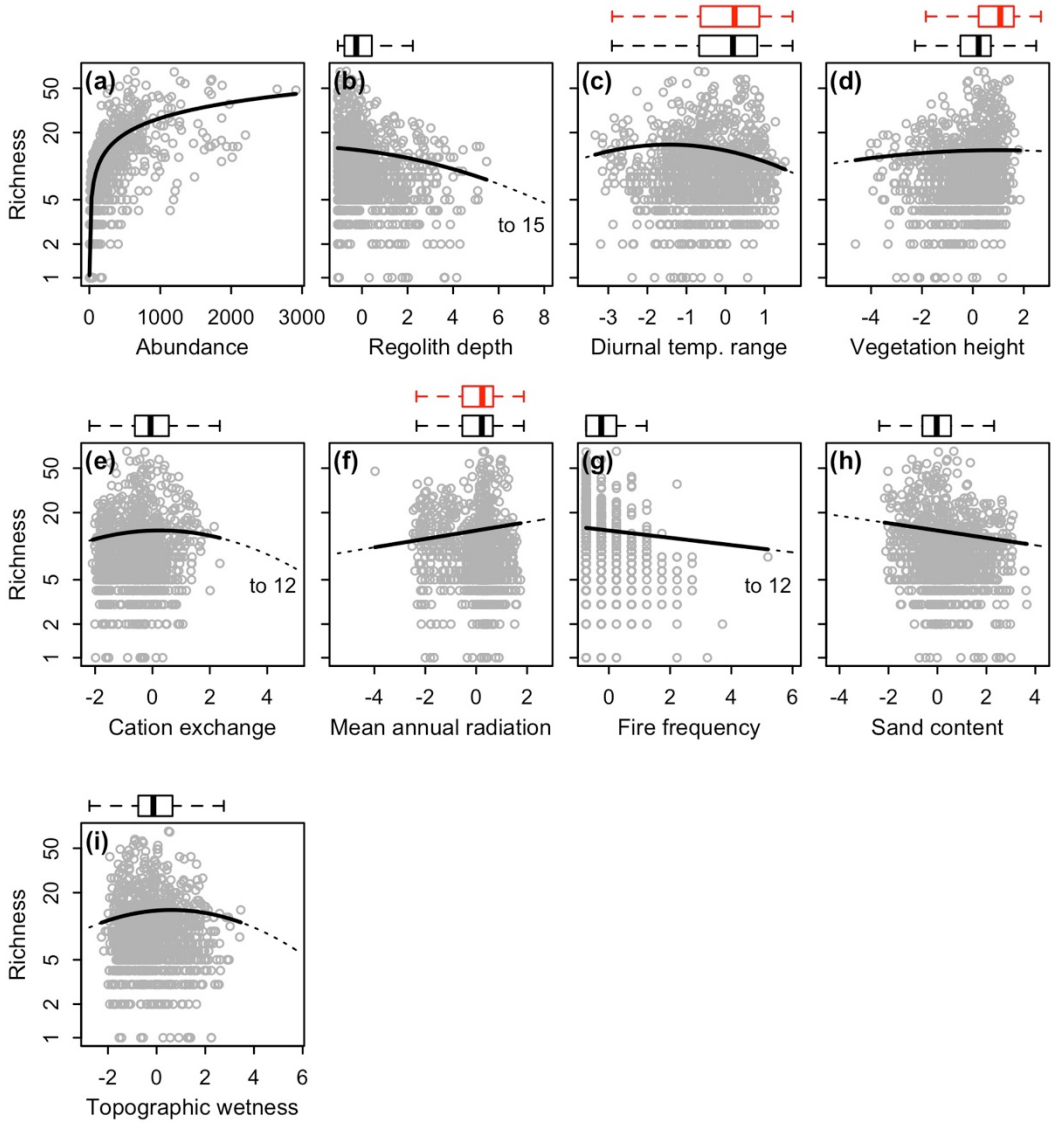

Figure A2. Abundance (a) and eight standardised predictor variables (b-i) were selected for the richness model. The solid lines are fitted relationships within sampled environmental space. Dotted lines extend into unsampled climate space. Box plots (outliers not shown) show the distribution of predictor variables under current (black) and future (red, where appropriate) climates. Note that future climate variables are clamped at the extremes of their current versions to reduce predicting into unsampled environmental space (see main text). Abundance and richness values indicate the number of stems/species per 1000 m^2 plot. The solid lines are fitted relationships. Richness values (the y-axis) are plotted on the $\log_e$ scale to aid interpretation.

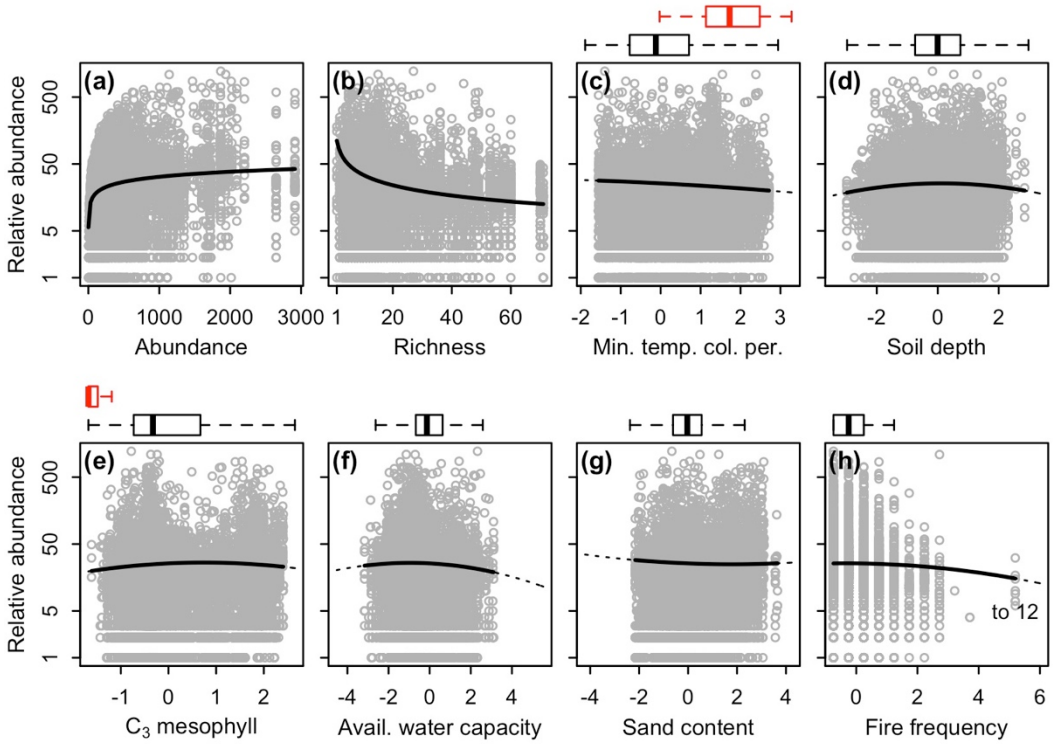

Figure A3. Abundance (a), richness (b) and six standardised predictor variables were selected for the evenness model. The solid lines are fitted relationships within sampled environmental space. Dotted lines extend into unsampled climate space. Box plots (outliers not shown) show the distribution of predictor variables under current (black) and future (red, where appropriate) climates. Note that future climate variables are clamped at the extremes of their current versions to reduce predicting into unsampled environmental space (see main text). Abundance and richness values indicate the number of stems/species per 1000 m^2 plot and relative abundance are the number of individuals per species, per site. Relative abundance values (the y-axis) are plotted on the $\log_e$ scale to aid interpretation.

Appendix 8. Mean predictions and coefficient of variations (CVs) for current and future RAD components.

The three RAD models were reasonably effective at predicting the three RAD components although there was a degree of scatter in the abundance model (Figure A1). Cross-validation showed that the random removal of 10% of the sites did not generally reduce the performance of the models (Figure A1). When projected spatially, our predictions of abundance, richness and evenness were reasonably accurate across the 500 bootstraps on the predictions implemented in this study (Figure A2, Table A1). Although some of the CV values may seem significant, the scale at which we are working is heavily log distributed (with predicted site-level abundances ranging from 34 to 23,585 species) so the patterns when assessed at a broad scale remain valid. Previous studies implementing this RAD modelling technique implemented 10,000 bootstrap predictions (Dunstan & Foster 2011; Dunstan et al. 2012; Leaper et al. 2012). Increasing the number of bootstraps implemented in this study would have lowered these CV values however, as we were working at a much greater resolution than these previous studies (90 m vs. 1,000 m), we had a significantly greater number of grid cells to predict across and increasing the number of bootstraps was not possible given present computational restrictions. As we implemented here, 500 bootstraps took ten days using a computer cluster with 76 virtual central processing units (CPUs), effectively 18,240 CPU hours (2.1 CPU years).

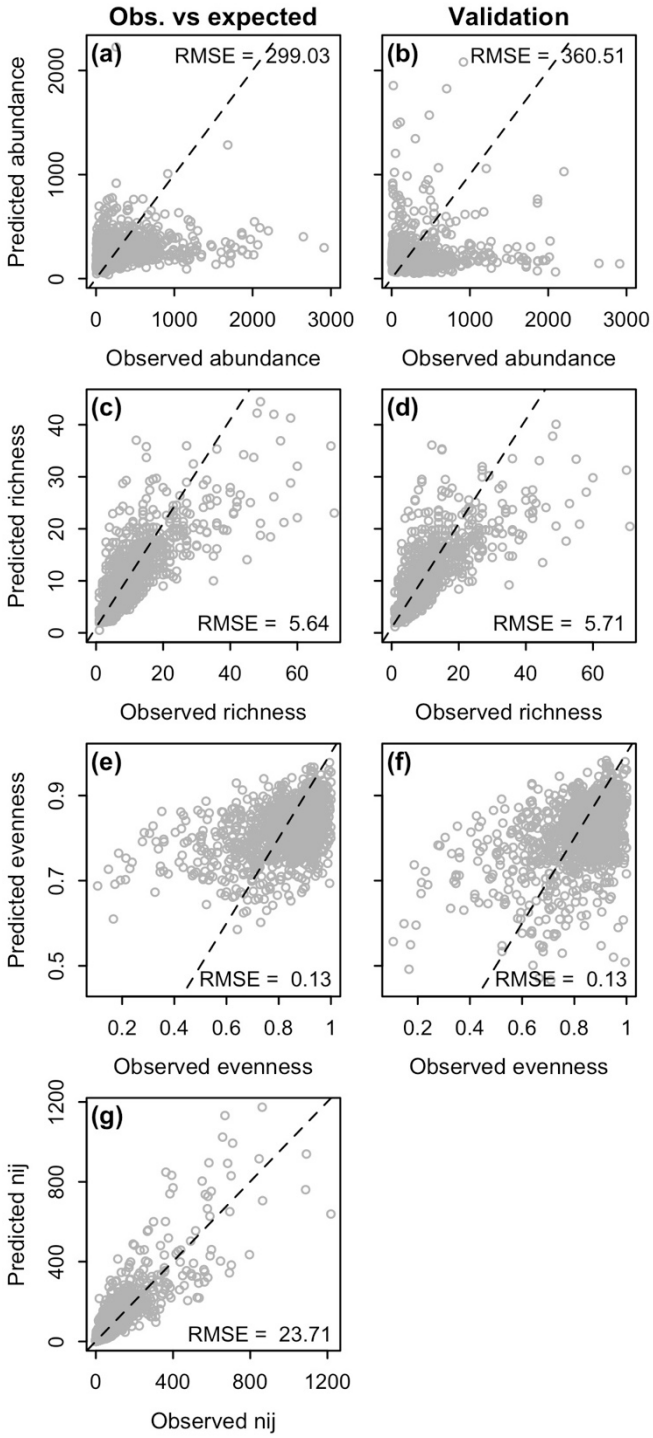

Figure A1. Results of our cross-validation exercise assessing accuracy and performance of the three RAD model components (abundance, richness and evenness) with variation between observed and predicted data reported as root mean square error (RMSE). Plots in the first column ("Obs. vs expected") show the relationship between observed and predicted values of (a) total abundance, (c) total richness, (e) Pielou's evenness and (f) individual species abundances. Plots in the second column ("Validation") show the results of the cross-validation exercise for the (b) abundance, (d) richness and (c) evenness RAD models. The dashed, diagonal lines follow the 1:1 relationship between observed and predicted values.

Note that it is not possible to present a comparison of species abundance values from the cross-validation exercise as the sequential nature of the RAD modelling technique means that richness values will usually differ slightly from those observed.

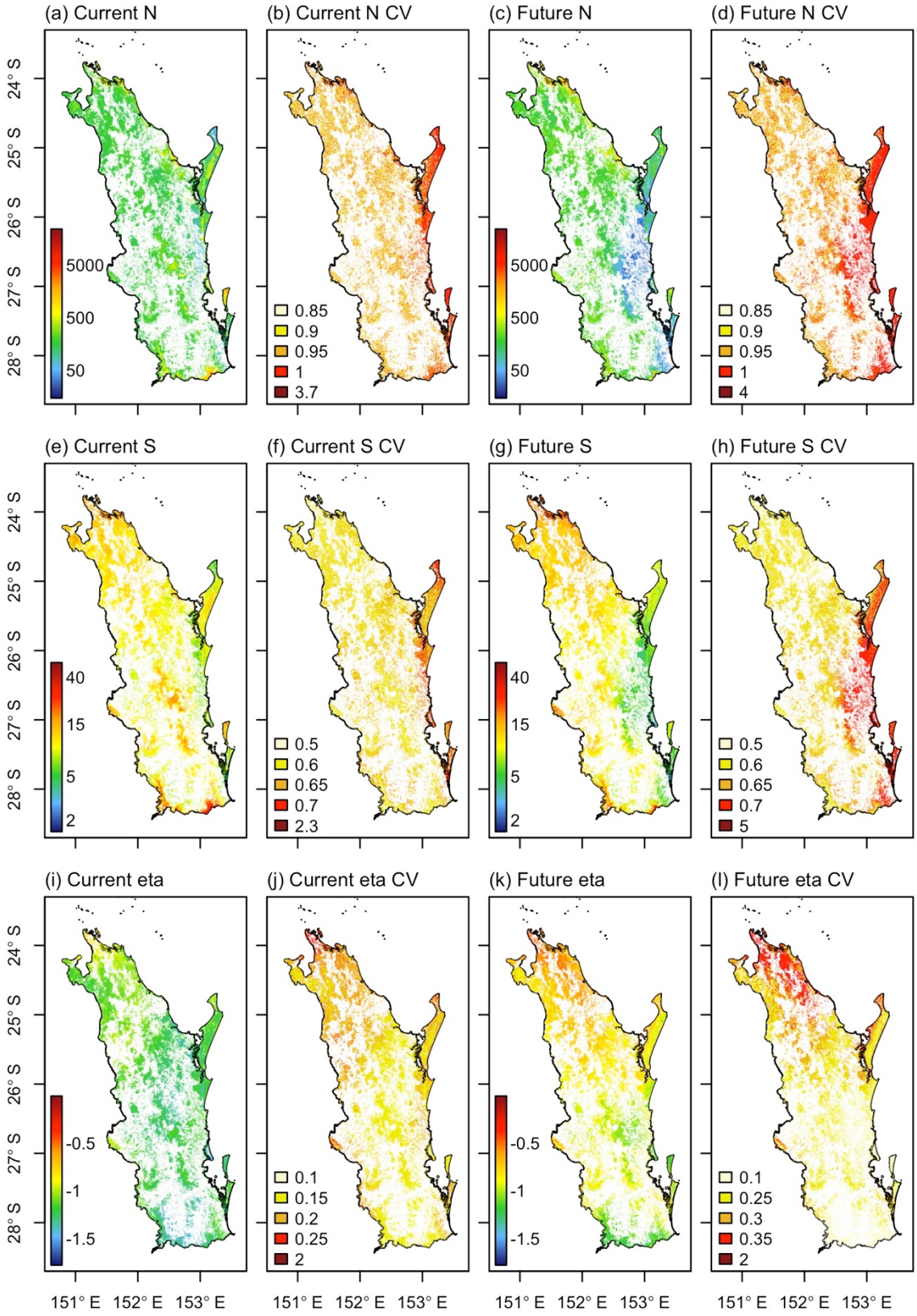

Figure A2. Mean predictions and associated coefficients of variation (CV) of abundance (a-d, N), richness (e-h, S) and evenness (i-l, eta) under current and future climates. Note that

abundance and richness are plotted on the $\log_e$ scale to aid interpretation. Colour scales on the CV plots are non-linear to avoid loss of colour delineation driven by extreme outliers (in most cases, CVs of > 1).

Table A1. Mean and median coefficient of variation (CV) values for the predicted RAD distributions across SEQ under current and future climate conditions.

	Current conditions		Future conditions	
RAD component	Mean	Median	Mean	Median
Abundance	0.95	0.94	0.99	0.97
Richness	0.64	0.64	0.65	0.65
Evenness	0.20	0.20	0.29	0.28

Appendix 8 references

Dunstan, P. K. and Foster, S. D. 2011. RAD biodiversity: Prediction of rank abundance distributions from deep water benthic assemblages. — Ecography 34: 798-806.

Dunstan, P. K. et al. 2012. Identifying hotspots for biodiversity management using rank abundance distributions. — Divers. Distrib. 18: 22-32.

Leaper, R. et al. 2012. Comparing large-scale bioregions and fine-scale community-level biodiversity predictions from subtidal rocky reefs across south-eastern Australia. — J. Appl. Ecol. 49: 851-860.

Environmental variable	Broad category	Unit	Short description	Reference
Prescott's index	Climate	No unit	A measure of water balance where larger values indicate wetter conditions.	Gallant & Austin (2012a)
Regolith depth	Substrate	m	The depth of soil before hard rock is encountered.	Wilford et al. (2015)
Sand content	Substrate	%	The sand content of the surface soil (0-50 mm).	Viscarra Rossel et al. (2014g)
Silt content	Substrate	%	The silt content of the surface soil (0-50 mm).	Viscarra Rossel et al. (2014h)
Soil bulk density	Substrate	g/cm^3	The whole bulk density of the surface soil (0-50 mm, including coarse fragments).	Viscarra Rossel et al. (2014i)
Soil carbon content	Substrate	tonnes/ha	The organic carbon content of the surface soil (0-300 mm).	Viscarra Rossel et al. (2014j)
Soil depth	Substrate	m	The depth of the soil profile (A and B horizons).	Viscarra Rossel et al. (2014k)
Temperature annual range	Climate	°C	The difference between the maximum temperature of warmest period and the minimum temperature of coldest period.	Xu & Hutchinson (2011)
Temperature isothermality	Climate	No unit	The mean diurnal range divided by the annual temperature range with high values indicating less variable annual temperatures.	Xu & Hutchinson (2011)
Temperature seasonality	Climate	Coefficient of variation	The standard deviation of the weekly mean temperatures expressed as a percentage of the mean of those temperatures using degrees Kelvin.	Xu & Hutchinson (2011)
Topographic wetness index	Substrate	Index	An index which estimates the relative wetness within a catchment	Gallant & Austin (2012b)
Vegetation height	Vegetation	m	The median height of the tallest stratum.	Appendix 4
Weathering intensity index	Substrate	Index	Index from low (largely un-weathered landscapes with a high proportion of fresh bedrock) to high (extremely weathered landscapes where the bedrock is completely weathered to secondary minerals).	Wilford (2012)